Field-induced rotational autoionization of Li_2

C. R. Mahon, G. R. Janik,* and T. F. Gallagher
Department of Physics, University of Virginia, Charlottesville, Virginia 22901
(Received 12 October 1989)

We have studied electric-field-induced rotational autoionization of Li_2 Rydberg states converging to high, $R > 10$, rotational limits of the Li_2^+ ion. Although autoionization of such states lying above the lowest rotational level of Li_2^+ is energetically allowed, the process is inhibited by the large transfer of angular momentum required from the ion core to the exiting electron, and it, in theory, does not occur in zero field. Nonetheless, autoionization requiring the transfer of ~ 10 units of angular momentum is readily observed in fields of 10–330 V/cm. The application of a field allows autoionization to occur to the nearest continuum by allowing a series of quadrupole transitions, in each of which the molecular ion core loses two units of angular momentum while the Rydberg electron's angular momentum is unchanged. We present a quantitative model based on this mechanism that is in satisfactory agreement with our experimental results.

I. INTRODUCTION

In many ways a diatomic molecule is similar to an atom. However, the additional rotational and vibrational degrees of freedom lead to interesting differences. For example, the existence of rotational levels of the diatomic ion implies that there are many low-lying ionization limits in a diatomic molecule, in marked contrast to atomic systems. The existence of so many low-lying ionization limits raises several questions. For example, how does electric field ionization occur for Rydberg states converging to excited rotational levels of the ion? Similarly, Rydberg states converging to higher rotational levels of the ion can, in principle, autoionize to the lowest rotational level of the ion, but the process requires the transfer of many units of angular momentum from the core to the ejected electron. Does this process occur at an observable rate? Fortunately, the higher rotational levels of the ground electronic state of alkali-metal dimers are thermally populated, and using laser excitation we can prepare Rydberg states converging to excited rotational levels of the ion to address these questions experimentally.

The first of the above questions has already been answered. Field ionization of a diatomic molecule is similar to field ionization in a complex atom, i.e., the phenomenon of forced autoionization occurs.[1–3] The basic notion is straightforward. An electric field depresses each ionization limit by $\Delta W = -2\sqrt{E}$ (we use atomic units unless otherwise stated). To a first approximation all states, regardless of the limit to which they converge, lying above the depressed lowest ionization limit can autoionize into the Stark-induced continuum above this limit, and this limit therefore determines the field ionization threshold for the molecule. Since ionization occurs almost irrespective of the quantum numbers of the state in question, it is often the case that low n states converging to rotationally (or vibrationally) excited levels of the ion are ionized by apparently impossibly weak fields. For example, Rydberg molecules with principal quantum number $\simeq 20$ have been ionized in a field of ~ 100 V/cm. The exceptions to the above rule, which is based solely on energy, are states converging to high rotational levels of the ion, bringing us to the second of the above questions. Bordas *et al.*[4,5] have observed that Rydberg states converging to high rotational states of the ion do not automatically ionize; the required angular momentum transfer from the ion to the electron is apparently too great.

The existence of an angular momentum impediment to rotational autoionization involving the transfer of many units of angular momentum is hardly surprising. Our estimate of the rate of autoionization of a state converging to an $R = 20$ rotational level of the ion to the $R = 0$ level is 10^{-55} s^{-1}. Here R is the rotational angular momentum quantum number of the diatomic Li_2^+ ion core. Even when only ten units of angular momentum are exchanged the calculated rate is unobservably small, 10^{-16} s^{-1}, yet in the presence of small electric fields such autoionization processes are observed, implying autoionization rates of $> 10^6$ s^{-1}, as first noted by Eisel and Demtröder.[6] Bordas *et al.*[4,5] have suggested that the field allows autoionization to occur by a series of quadrupole couplings with $\Delta R = -2$, and $\Delta l = 0$, where l is the orbital angular momentum of the Rydberg electron. In zero field the quadrupole couplings must be $\Delta R = -2$ and $\Delta l = +2$. This series of couplings, via very nearly degenerate intermediate states, connects the Rydberg states converging to a high rotational level of the ion to the continuum above the ground rotational level of the ion.

Here we present the results of a quantitative experimental study of the effect of electric fields on the ionization of rotationally and vibrationally excited Li_2 molecules, with particular attention to the cases in which the presence of the electric field allows large amounts of angular momentum to be transferred from the ion core. The experimental results are then compared to a quantitative model based on the mechanism first suggested by

Bordas *et al.*[4,5] which gives reasonable predictions of the threshold fields for ionization, even in the case of Rydberg states converging to high rotational levels of the ion.

II. EXPERIMENTAL METHOD

The experiments are conducted using two-step pulsed laser excitation of Li_2 molecules in a supersonic beam. The molecules in the beam are in the ground X electronic state, the ground vibrational level $v''=0$, and in a range of J'' rotational levels. With the first laser, at $\lambda \sim 670$ nm, we drive the transition to the electronically excited A state. Due to the displacement of the minima of the potential curves of the X and A states it is possible to drive transitions from the $v''=0$ level of the X state to several v' levels of the A state. However, since both the X and A states are Σ states, only $P(\Delta J=-1)$ and $R(\Delta J=1)$ transitions are possible, and the A state rotational quantum number $J'=J''\pm 1$. By choosing the wavelength of the $A \leftarrow X$ transition we can easily excite a single $v'J''$ level of the A state from the range of J'' levels that are populated in the Li_2 beam. The second laser drives the 370-nm transition from the $v'J'$ level of the A state to the final Rydberg state. Since the A state potential has a minimum at the same internuclear separation as that of the Li_2^+ ground state, and nearly the same shape, only $\Delta v=0$ transitions are allowed, and the vibrational level of the Rydberg state $v=v'$. The Rydberg states are either Σ or Π states, and as a result the total angular momentum $J=J'$ or $J'\pm 1$. In a Rydberg state J is the sum of the angular momentum R of the Li_2^+ core added to the angular momentum l of the outer electron, which is in an s or d state since we are using electric dipole excitation from the A state which has strong $2p$ character. In sum we can produce Li_2 Rydberg states with the Rydberg electron in a state of $l \leq 2$, and the Li_2^+ core in a rotational level R which we choose by our choice of J' in the A state. We detect the Li_2^+ ions resulting from the autoionization of the Rydberg molecules.

Since the apparatus has been described before,[2] our description here is brief. The Li_2 beam is generated by heating a 3.2-cm-diam, 10-cm-long stainless-steel oven, fitted with a removable nozzle with a 0.6-mm-diam orifice. The oven is surrounded by an electrically isolated 12-μm-thick molybdenum foil heating element which carries a typical current of 150 A, producing a temperature of 1100 K. To forestall the formation of clogs the nozzle is separately heated to a temperature slightly in excess of the oven's by a coaxial nichrome heater. Based on the observed $A \leftarrow X$ bands at an oven heater current of 150 A the resulting Li_2 beam has vibrational and rotational temperatures of ~ 200 and 300 K.

The 670- and 370-nm laser beams are generated by pumping two dye lasers with the 532-nm second harmonic of a Q-switched Nd:YAG (yttrium aluminum garnet) laser operating at a 10-Hz repetition rate. The 670-nm laser is a simple Littman-type oscillator, with $\simeq 0.3$ cm^{-1} linewidth and 100-μJ pulse energies. The 370-nm beam is generated by mixing the 560-nm output of a Quanta-Ray PDL-1 oscillator-amplifier dye laser with the residual 1064-nm Nd:YAG laser beam in a potassium dihydrogen phosphate KDP crystal. At 370 nm the linewidth is $\simeq 1$ cm^{-1} and typical pulse energies are ~ 10 μJ. The two parallel laser beams intersect the Li_2 beam at right angles between two electric field plates 2.34 cm apart, and the Li_2^+ ions resulting from autoionization are accelerated through a screened hole in the top field plate by a dc voltage applied to the bottom plate. The ions are detected by a particle multiplier positioned above the interaction region, and the multiplier signal is recorded by a gated integrator with a gate width of 100 ns, positioned so as to detect signals from ions produced in the 100 ns immediately following the laser pulses. This arrangement sets a lower limit of 10^7 s^{-1} on the autoionization rates for the Rydberg states detected.

III. OBSERVATIONS

Most of our data are in the form of excitation spectra obtained by recording the Li_2^+ signal as the wavelength of the second laser is scanned. In Fig. 1 we show the spectra obtained in fields of 10 and 100 V/cm from the $v'=0$, $J'=13$ level of the A state, and in Fig. 2 spectra in

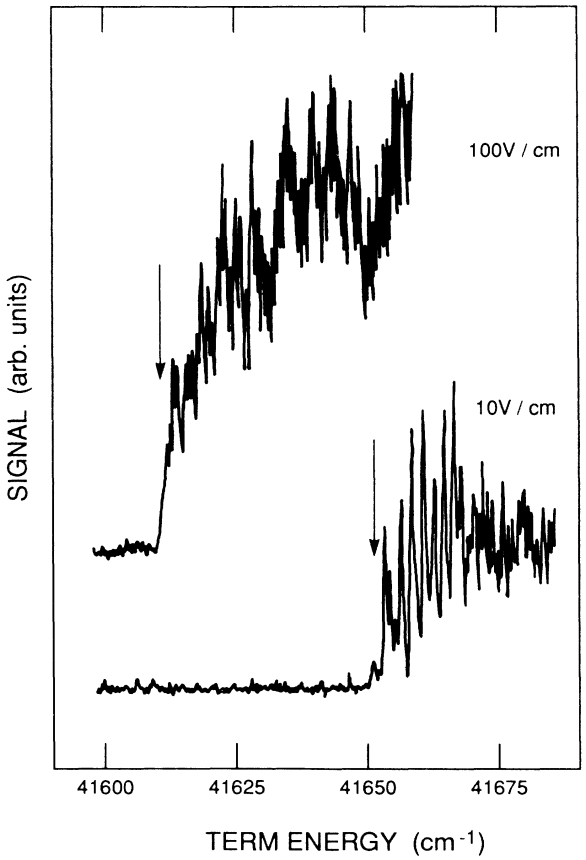

FIG. 1. Autoionization spectra for static fields of 10 and 100 V/cm for which the ionization threshold corresponds to the Stark depressed ground state of the ion, $v=0$, $R=0$. The intermediate state is the $v=0$, $J'=13$ A state. The depression of the ionization limit can be accounted for completely by forced autoionization.

fields of 10, 100, and 330 V/cm from the $J'=23$ level of the A state. The horizontal axes of Figs. 1 and 2 are expressed as the term energy, measured from the bottom of the ground, X, state potential well. As shown by Figs. 1 and 2 we observe a signal only when the term energy W exceeds a threshold energy W_{th}, shown by the arrows, above which the autoionization rate exceeds $10^7\ s^{-1}$. It is apparent that the threshold energy decreases as the electric field is increased. The depression of the threshold energy is due to two effects. The first is forced autoionization. The field depresses the ionization limits by ΔW, given, in atomic units, by

$$\Delta W=-2\sqrt{E}\ . \tag{1}$$

All rotational limits are depressed by the same amount, and in Fig. 1 we show the field depressed limits corresponding to $v=0$ rotational levels of Li_2^+. Explicitly these $v=0$ limits are given by

$$I(R)=I(0)+B_0R(R+1)-2\sqrt{E}\ . \tag{2}$$

Here $I(0)=41671\ cm^{-1}$ is the zero-field $R=0$ ionization limit of Li_2^+, and $B_0=0.493\ cm^{-1}$ is the $v=0$ rotational constant of Li_2^+.[7]

In Fig. 1 the threshold energies correspond to the depressed $R=0$ ionization limits given by Eq. (2). In other words, forced autoionization alone is an adequate explanation of the results, as has been previously shown by Janik *et al.*[2] In Fig. 2, however, it is apparent that W_{th} does not correspond to the depressed $R=0$ limit, but to the $R=13$ and 8 limits for fields of 10 and 100 V/cm. Only in a field of 330 V/cm does W_{th} occur at the $R=0$ limit. Autoionization to the $R=0$ ionic level does not occur in the fields of 10 and 100 V/cm because the molecule cannot transfer the angular momentum from the molecular ion core to the departing electron. Autoionization to progressively lower rotational states of the ion occurs as the field is increased is due to field-induced rotational autoionization, the second contribution to the depression of W_{th}.

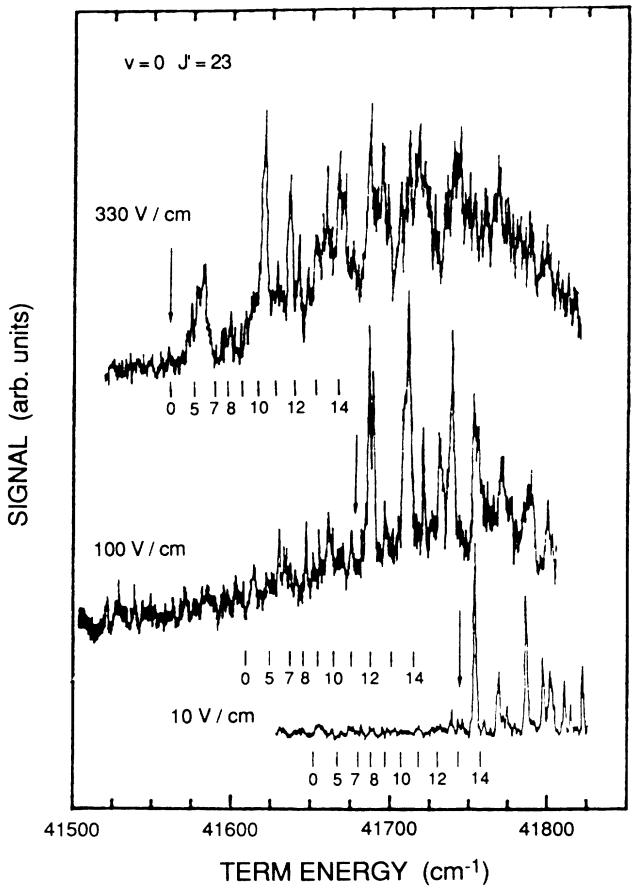

FIG. 2. Autoionization spectra with the first laser tuned to the $v=0$, $J'=23$ A state for static fields of 10, 100, and 330 V/cm. Included are the positions of the Stark depressed $v=0$, R levels of Li_2^+. The energy thresholds for autoionization are taken as the onset of signal in the spectra, indicated by the vertical arrows at $R=13$, 11, and 0, respectively. The depression of the ionization threshold is due to two field effects. The first is forced autoionization, and the second is field-induced rotational autoionization.

To obtain a complete picture of this phenomenon, we have recorded spectra analogous to those shown in Figs. 1 and 2 for Rydberg states converging to many rotational levels of the $v=0$ and 1 vibrational levels of the Li_2^+ ion core. In Table I we tabulate the threshold energies observed for the $v=0$ Rydberg states excited from intermediate A state $v=0$ levels with $13\le J'\le 33$. We also list in Table I the measured values for R_{th}, the value of R at W_{th}. The 330 V/cm data of Table I show that molecular Rydberg states with angular momentum $J\le\sim 20$ all autoionize to the ground state of the ion, while higher angular momentum states autoionize to rotationally excited ion levels. For $J'=34$ and a static field of 10 V/cm, the core and Rydberg electron cannot exchange more than four units of angular momentum during the autoionization process, while increasing the field from 10 to 300 V/cm facilitates the exchange of an additional ~ 13 units of angular momentum.

Although our primary interest is pure rotational autoionization, we have also recorded analogous spectra of Rydberg states converging to $v=1$ rotational levels of Li_2^+ via $v=1$ levels of the A state. Of particular interest are states which undergo vibrational-rotational autoionization. In Fig. 3 we show spectra obtained via the $v'=1$, $J'=30$ level of the A state. For reference we have shown the ionization limits of $v=0$ rotational levels of Li_2^+ as well as the location of the unperturbed levels converging to the $v=1$, $R=29$ and 31 levels of Li_2^+. The Rydberg series converging to the $v=1$ levels of the ion core are of low enough n that the Rydberg series is evident even in the presence of a field of 330 V/cm. In Table II we present the values of W_{th} and R_{th} obtained for the Rydberg states converging to the $v=1$ states of the ion.

An alternative, complementary method of recording the data is to monitor the Li_2^+ signal as the field is varied with the second, Rydberg$\leftarrow A$, laser tuned to a Rydberg state. In this case we determine threshold fields for ionization instead of energies. We use the $v=1$ states

TABLE I. Measured $v=0$ autoionization threshold term energies W_{th} and the corresponding $v=0$ R ion limits at threshold.

$v=0$ state	10 V/cm		100 V/cm		330 V/cm	
J'	R_{th}	W_{th} (cm^{-1})	R_{th}	W_{th} (cm^{-1})	R_{th}	W_{th} (cm^{-1})
10	0	41 652(3)	0	41 610(2)		
13	0	41 652(3)	0	41 610(2)		
16	4	41 662(3)	0	41 610(2)		
17	0	41 652(3)	0	41 610(2)		
18	4	41 662(3)	0	41 610(2)		
19			0	41 610(2)		
20	8	41 688(4)	0	41 610(2)		
21	10	41 706(5)	5	41 625(3)		
23	13	41 742(7)	8	41 646(4)	0	41 560(2)
24	13	41 742(7)	9	41 654(5)		
26	17	41 802(8)	9	41 654(5)	7	41 588(4)
29	20	41 858(10)	17	41 760(9)		
30	22	41 900(11)	14	41 713(7)	12	41 637(3)
31	23	41 922(11)	19	41 797(9)		

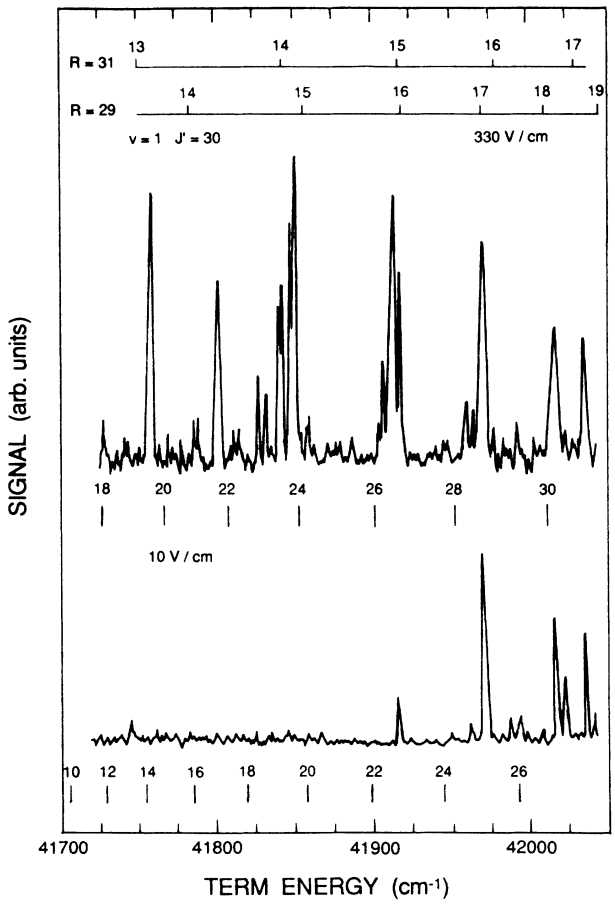

FIG. 3. $v=1$ autoionization spectra with the first laser tuned to the $v=1$, $J'=30$ A state for 10 and 330 V/cm static fields. Included for reference are the positions of the unperturbed $v=1$, $R=29d\pi$ and $R=31d\pi$ Rydberg series, as well as the Stark depressed limits of the $v=0$, R levels of Li_2^+.

which, being lower in n than degenerate $v=0$ states of the same R, autoionize in fields so low that no Stark shifts are evident. In Fig. 4 we show three examples. The first laser is tuned to excite the $v'=1$, $J'=30$ level of the A state and the second laser is tuned to energies of 41 849, 41 799, and 41 755 cm^{-1}. We assign these three features as, respectively, $(R,n)=(29,15;31,14)$, (27,15), (31,13). As the electric field is increased we observe in each case a sharp increase in the ionization signal, at 77, 119, and 142 V/cm, respectively, which we term the threshold fields. It is interesting to note that all three levels lie above the $R=0$, $v=0$ ionization limit, so in this case it is evident that the sole role of the field is to overcome an angular momentum impediment to autoionization. In Table III we list the measured threshold fields for $v=1$ Rydberg states obtained from spectra from the $v'=1$, $J'=21$, 26, and 30 levels of the A state.

IV. THEORY

In this section we first show that the zero-field rotational autoionization of Rydberg states converging to high rotational levels of the ion to low rotational levels of the ion is unobservable. Second we show how this pro-

TABLE II. Measured $v=1$ autoionization threshold term energies W_{th} and the corresponding $v=0$ R ion limits at threshold

	10 V/cm		330 V/cm	
J'	R_{th}	W_{th} (cm^{-1})	R_{th}	W_{th} (cm^{-1})
21	15	41 770(8)	0	41 560(10)
26	17	41 802(9)	0	41 560(10)
30	22	41 900(11)	15	41 696(10)

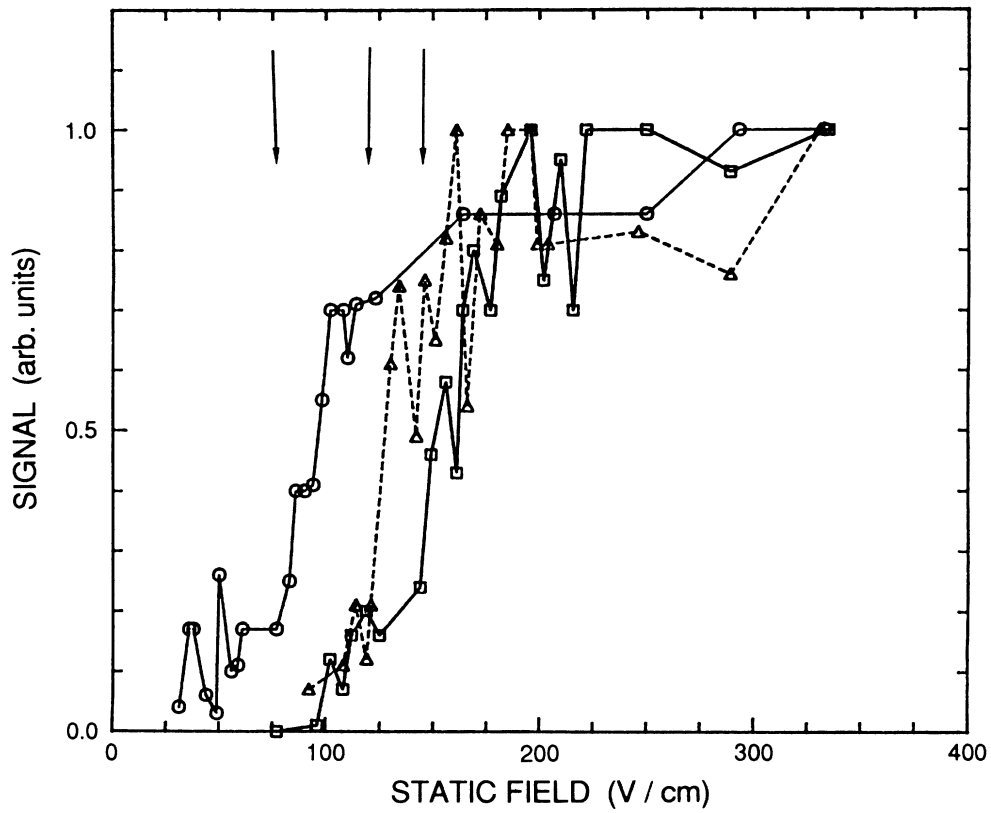

FIG. 4. Autoionization signal as a function of the applied static field with the first laser tuned to the $J'=30$, $v=1$ A state, and the second laser tuned to the $(R,n)=(31,14)$ (circles), (29,14) (triangles), (31,13) (squares) states. The thresholds for autoionization, indicated by the vertical arrows, are taken as the points at which the ion signals sharply increase.

TABLE III. Measured autoionization threshold fields F_{th} with the second laser tuned to $v=1$ (R,n) Rydberg states with term energies W.

J'	(R,n) $d\pi$ state, term energy (cm^{-1})	Threshold field (V/cm)
21		
	(22,15)	18.5±1.0
	41689	
26		
	(27,14)	51.8±2.8
	41740	
	(25,14)	142±4
	41693	
	(27,13)	119±4
	41649	
	(26,13)	172±4
	41622	
30		
	(31,14)	76.6±3.6
	41849	
	(29,14)	123±4
	41799	
	(31,13)	144±5
	41755	

cess is allowed by the application of quite small fields. Finally, using a simple model based on the above understanding, we compare predictions for threshold energies and fields for autoionization to the experimental observations.

We begin by considering the zero-field autoionization of Li_2 Rydberg states converging to the rotational levels of the ground vibrational level of Li_2^+. In Fig. 5 we show the even $R=0$ to 12 ionization limits. For simplicity we ignore the spins of the electrons and describe the Li_2 Rydberg molecule as an electron of angular momentum l slowly circulating in a large orbit about a rapidly rotating Li_2^+ core of angular momentum R. The total angular momentum is thus $\mathbf{J}=\mathbf{l}+\mathbf{R}$. In zero field, states of the same total angular momentum J are coupled by the even electrostatic multipole interactions between the Li_2^+ core and the valence electron, and this coupling leads to rotational autoionization. Since Li_2^+ is homonuclear, the odd multipole interactions vanish. For this reason we have shown only even values of R in Fig. 5. However, we could equally, well have shown only odd values of R.

In general the autoionization rate Γ from a state of quantum numbers R, n, l, and J to the continuum of energy ε' above the R' rotational level of the ion is given by

$$\Gamma=2\pi|\langle RnlJ|V|R'\varepsilon'l'J\rangle|^2 , \quad (3)$$

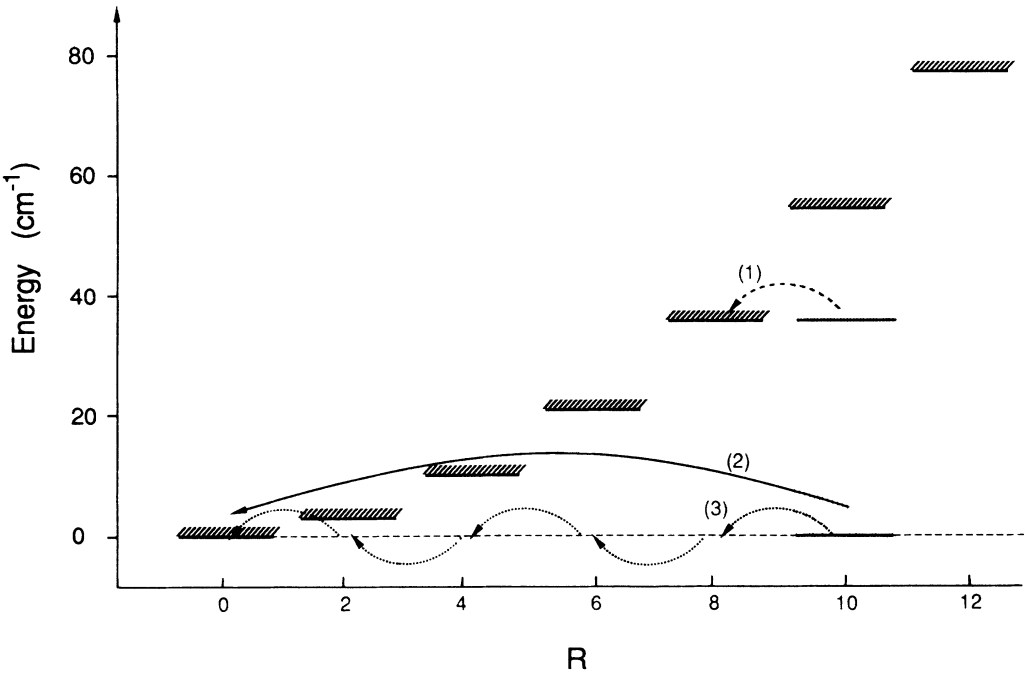

FIG. 5. Schematic showing the positions of the $R=0$–12, $v=0$ limits of Li_2^+ relative to the lowest $v=0$, $R=0$ limit. Rydberg states converging to the $R=10$ limit that lie above the $R=8$ limit may autoionize by a single $\Delta R=-2$, $\Delta Rl=+2$ quadrupole transition with observable rate $>10^7\ s^{-1}$ [path (1)]. Lower-lying states just above the $R=0$ limit may autoionize to the $R=0$ continuum essentially in two ways. The first is via their $\Delta R=-2$, $\Delta l=+2$ quadrupole couplings with the nearly degenerate states of the four intermediate Rydberg series [path (3)]. The second is the direct 2^{10}-pole, $\Delta R=-10$, $\Delta=+10$ process [path (2)].

where the continuum wave function is normalized per unit energy. The most rapid rate for autoionization is usually via the lowest multipole interaction, which is the quadrupole interaction in this case. An example of quadrupole autoionization is shown by process (1) in Fig. 5, the autoionization of a Rydberg state converging to the $R=10$ limit to the continuum above the $R=8$ limit. Quadrupole autoionization in a homonuclear diatomic molecule has been worked out in detail by Eyler and Pipkin,[8] and an analogous description of dipole and quadrupole autoionization, as would be observed in a heteronuclear molecule has been given by Jaffe *et al.*[9] We shall consider a simplified version of the quadrupole treatment which gives good order-of-magnitude values and serves as an adequate starting point for the calculation of field effects.

Consider an $l=2$ Rydberg state converging to the R level of Li_2^+. If it lies above the $R-2$ limit it can autoionize to the $R-2$ level of the ion by $\Delta l=2$, 0, and -2 quadrupole interactions. If we assume that the Rydberg electron remains outside the Li_2 core, the interaction matrix element may be written as

$$\langle RnlJ|V|R-2\,\varepsilon' l'J\rangle \simeq \tfrac{1}{3}\langle R|r_{\rm ion}^2|R-2\rangle\left\langle nl\left|\frac{1}{r^3}\right|\varepsilon' l'\right\rangle . \tag{4}$$

In writing Eq. (4) we have replaced the explicit J dependence with the factor $\frac{1}{3}$. The quadrupole matrix element of the ion is, to a reasonable approximation, 18 in atomic units.[10] For $n\gg l$ we generalize the expectation values for $1/r^3$ (Ref. 11) to write approximate bound-bound $1/r^3$ matrix elements for the outer electron as

$$\left\langle nl\left|\frac{1}{r^3}\right|n' l\right\rangle = \frac{1}{n^{3/2}}\frac{1}{n'^{3/2}}\frac{1}{(l+1/2)^3}\ , \tag{5}$$

$$\left\langle nl\left|\frac{1}{r^3}\right|n' l+2\right\rangle \simeq \frac{1}{30}\frac{1}{n^{3/2}}\frac{1}{n'^{3/2}}\frac{1}{(l+5/2)^3}\ . \tag{6}$$

In rotational autoionization the electrons are ejected with very low energies, and we can obtain the bound-free $\varepsilon\simeq 0$ matrix element, for a continuum wave normalized per unit energy, by simply removing the factor of $n'^{3/2}$ from the bound-bound matrix elements of Eqs. (5) and (6). For example,

$$\left\langle nl\left|\frac{1}{r^3}\right|\varepsilon l\right\rangle = \frac{1}{n^{3/2}}\frac{1}{(l+\frac{1}{2})^3}\ . \tag{7}$$

Using Eqs. (4)–(7) we can see that quadrupole autoionization proceeds at rates of $\sim 230n^{-3}(l+\frac{1}{2})^{-6}$ for $l\to l$ and $0.25n^{-3}(l+\frac{5}{2})^{-6}$ for $l\to l+2$. For $n=25$ and $l=2$ these rates are 6×10^{-5} and 2×10^{-9}, or, converting from atomic units to s^{-1}, 2×10^{12} and $8\times10^{7}\ s^{-1}$. Both of these rates are in excess of the rate of $10^7\ s^{-1}$ required for detection by our experiment, but the $l\to l+2$ rate is 4 orders of magnitude slower. We note that for ejected elec-

trons with very low energy the $\Delta l=0$ rates are rapid, while at higher ejected electron energies the $\Delta l=2$ rates are more rapid.

Our primary interest here is in the optically accessible Rydberg states of low l converging to high rotational levels of the Li_2^+ ion but lying above only very low rotational limits. Such Rydberg states can autoionize either by a direct multipole interaction or by a series of quadrupole interactions through virtual intermediate states. In Fig. 5 these two possibilities for a Rydberg state converging to the $R=10$ limit are shown by processes (2) and (3), respectively. We consider as an example the autoionization of an $l=2$ Rydberg state converging to the ion limit R to the $R-10$ level of the ion. The direct multipole process has a typical matrix element

$$\langle Rn\,l=2|V|R-10\,\varepsilon\,l=12\rangle \simeq \langle R|r_{\rm ion}^{10}|R-10\rangle\left\langle n\,l=2\left|\frac{1}{r^{11}}\right|\varepsilon\,l=12\right\rangle . \quad (8)$$

The 2^{10}-pole matrix element of the ion is $\sim(18a_0^2)^5$ and the $1/r^{11}$ matrix element for the outer electron is $\sim 10^{-26}n^{-3}$. Together these yield an autoionization rate of $10^{-39}n^{-3}$. For $n=25$, this is a rate of $10^{-26}\ s^{-1}$, far too slow to be observed.

Now let us consider the alternative, a five-step quadrupole coupling through four intermediate states shown by process (3) in Fig. 5. The matrix element is given by fifth-order perturbation theory as a summation of products of matrix elements of the form

$$\begin{aligned}\langle Rnl|V|R-10\,\varepsilon\,l+10\rangle \sim \sum_{\substack{n_1,n_2\\ n_3,n_4}} & \frac{1}{3}\frac{\langle R|r_{\rm ion}^2|R-2\rangle\langle nl|1/r^3|n_1\,l+2\rangle}{W_{n_1}-W_n}\,\frac{1}{3}\frac{\langle R-2|r_{\rm ion}^2|R-4\rangle\langle n_1\,l+2|1/r^3|n_2\,l+4\rangle}{W_{n_2}-W_n}\\ &\times\frac{1}{3}\frac{\langle R-4|R_{\rm ion}^2|R-6\rangle\langle n_2\,l+4|1/r^3|n_3\,l+6\rangle}{W_{n_3}-W_n}\\ &\times\frac{1}{3}\frac{\langle R-6|r_{\rm ion}^2|R-8\rangle\langle n_3\,l+6|1/r^3|n_4\,l+8\rangle}{W_{n_4}-W_n}\\ &\times\frac{1}{3}\langle R-8|r_{\rm ion}^2|R-10\rangle\langle n_4\,l+8|1/r^3|\varepsilon\,l+10\rangle . \end{aligned} \quad (9)$$

We can approximate the summations by taking the most nearly resonant terms, in which case the average energy denominator $W_{n_i}-W_n\sim 1/4n_i^3$ is a quarter the spacing of the bound ith Rydberg series at principal quantum number n_i. Using the forms of Eqs. (5) and (6) for the bound-bound $1/r^3$ matrix elements it is apparent that the $n_i^{3/2}$ factors from adjacent matrix elements cancel the n_i^3 factors in the energy denominators. Thus the matrix element of Eq. (9) is given by

$$\langle Rnl|V|R-10\,\varepsilon\,l+10\rangle \sim \tfrac{1}{3}^5 18^5 4^4 \tfrac{1}{30}^5 \frac{n^{-3/2}}{[(l+\frac{5}{2})(l+\frac{9}{2})(l+\frac{13}{2})(l+\frac{17}{2})(l+\frac{21}{2})]^3} . \quad (10)$$

This leads to a rate of $10^{-29}n^{-3}$. For $n=25$ the matrix element of Eq. (10) implies an autoionization rate of $10^{-16}\ s^{-1}$. While this exceeds the rate for direct 2^{10}-pole autoionization, it is still far too slow to be observed.

The development between Eqs. (9) and (10) brings out an important point. Adding the ith quadrupole step adds a factor of $\sim\frac{4}{5}(l+2i+\frac{1}{2})^{-3}$ to the matrix element, reducing the rate by the square, $\sim 0.64(l+2i+\frac{1}{2})^{-6}$. This reduction is independent of n. For example, the second step in Eq. (10) reduces the autoionization rate by a factor $\sim 10^{-5}$. For this reason an autoionization process with more than one $\Delta l=2$ step does not have an observable rate.

Now let us consider the effect of applying an electric field. The field destroys l and J as good quantum numbers. We now assume that this is true for all intermediate Rydberg series between the initial state and the continuum. In the field the nl states are converted to Stark states which are linear combinations of the angular momentum states. While l is not a good quantum number in the field, its projection m on the field direction is. In the following discussion we assume that $m=0$, which is a reasonable approximation for states optically excited from low-lying states. To appreciate the effect of the field consider the five-step quadrupole ionization discussed above. If we denote the states by (Rnl), the zero-field autoionization described above can be viewed as the following sequence of transitions:

$$\begin{aligned}(R,n,l)&\rightarrow(R-2,n_1,l+2)\\ &\rightarrow(R-4,n_2,l+4)\\ &\rightarrow\cdots\rightarrow(R-10,\varepsilon l+10) .\end{aligned} \quad (11)$$

In the field the process goes through intermediate Stark states, which have the parabolic quantum number k instead of l and are linear combinations of l states,

$$\begin{aligned}(R,n,l)&\rightarrow(R-2,n_1,k_1)\\ &\rightarrow(R-4,n_2,k_2)\\ &\rightarrow\cdots\rightarrow(R-10,\varepsilon,k_\varepsilon) .\end{aligned} \quad (12)$$

In each of the $1/r^3$ matrix elements between two Stark states, k_i and k_{i+1}, the largest contribution comes from the low-angular-momentum parts of the components of the Stark states k, with matrix elements $l \rightarrow l$. The sequence of Eq. (12) may therefore be replaced by

$$\begin{aligned}(R,n,l) &\rightarrow (R-2,n_1,l) \\ &\rightarrow (R-4,n_2,l) \\ &\rightarrow . \rightarrow . \rightarrow (R-10,\varepsilon,l) \ . \end{aligned} \tag{13}$$

If we compare this to the chain of Eq. (11) we can see that the $l \rightarrow l+2$ matrix elements have been replaced by $l \rightarrow l$ matrix elements which are larger by a factor ~ 100. Now each additional quadrupole step introduces an additional factor of $\sim 24/(l+\frac{1}{2})^3$ to the overall matrix element.

When we rewrite Eqs. (9) and (10) using the Stark states there are two new aspects which must be taken into account. First the intermediate n_i Stark states are linear combinations of l states, with amplitudes of $\sim 1(n_i)^{1/2}$ from each l state. Second the energy denominators are reduced. While spacing between the l states is $1/n_i^3$ the spacing between Stark states is a factor of n_i smaller since there are n_i Stark states per $\Delta n_i = 1$ interval. As a result the energy denominators are reduced by a factor of n_i. Since the $1/(n_i)^{1/2}$ enters in two adjacent matrix elements in the numerator, the factor of $1/n_i$ in the energy denominator is canceled. Thus the effect of the field is simply to replace the $l \rightarrow l+2$ matrix elements by $l \rightarrow l$ matrix elements which are a factor of 100 larger. In other words, for each of the quadrupole steps in which the $l \rightarrow l+2$ matrix element is replaced by an $l \rightarrow l$ matrix element there is an increase of roughly 4 orders of magnitude in the autoionization rate.

We have until this point discussed the autoionization process as either $\Delta l = 0$ or $\Delta l = 2$ transitions of some arbitrary l state. Now let us consider the question of choosing a low l to characterize the process. The expression of Eq. (4) for the quadrupole interaction is valid only for the electron outside the Li_2^+ core, which has a radius of $\sim 5a_0$. This condition is met for l states for which the inner turning point lies at $r > 5a_0$, i.e., $l \geq 3$. Experiments on atomic autoionizing states show that the autoionization rates can be calculated accurately using expressions such as Eq. (4) as long as the Rydberg electron does not penetrate the ion core. Furthermore, for the low-l states for which penetration does occur, the autoionization rates are roughly equal to the rate of the lowest-l nonpenetrating state. Therefore we use $l = 3$ to calculate the rates. Each $\Delta l = 0$ step adds a factor of $24/(l+\frac{1}{2})^3$ to the matrix element. For $l = 3$ this factor is ~ 1, implying that for all practical purposes an arbitrary number of such steps may be involved without changing the autoionization rate. While this statement is an oversimplification, it does allow us to develop a criterion for the observability of autoionization.

Above we found that autoionization with a single quadrupole $\Delta l = +2$ step was observable, with a rate of $\sim 10^8\ s^{-1}$, in excess of the observability limit of $10^7\ s^{-1}$. It is, however, clear that a process involving two $\Delta l = +2$ steps is not observable. Thus we adopt as an observability criterion that one $\Delta l = +2$ transition is allowed. It will be from the Rydberg state converging to R to the Rydberg series converging to $R-2$. All subsequent transitions must, however, be $\Delta l = 0$ transitions, requiring that the $R-4$ Rydberg series be converted to Stark states at the energy of the original Rydberg state.

When are the Stark states a good description of a Rydberg series? We require that the l state responsible for the autoionization be mixed with other l states of the same n and that the Stark states be spread over the entire Δn interval. Both requirements are met when the field $E \geq 1/3n^5$. This is usually termed the Inglis-Teller limit since it is the point at which different n states are not resolved in an electric field.

Using this field criterion we can now derive the threshold energy for autoionization of the $n,l = 2$ Rydberg states converging to rotational level R of the ion. In Fig. 6 we show the R, $R-2$, and $R-4$ limits which are separated in energy by $\simeq 4B_0R - 2B_0$ and $4B_0R - 10B_0$.

In a field E the Inglis-Teller suppression of the $R-4$ limit is to $n_{R-4} = (3E)^{-1/5}$, which lies at an energy $1/2n_{R-4}^2$ below the $R-4$ limit. Taking into account the rotational energy separation of the R and $R-4$ limits the energy threshold for autoionization lies at energy

$$\Delta W_1 = 8B_0R - 4B_0 + \tfrac{1}{2}(3E)^{2/5} \tag{14}$$

below the zero-field R ionization limit.

Expressed in another way, for a state (R,n_R) with term energy W, the threshold field condition for the Inglis-Teller suppression of the $R-4$ limit is

$$I(0) + (R-4)(R-3)B_0 - W = \tfrac{1}{2}(3E)^{2/5} \ . \tag{15}$$

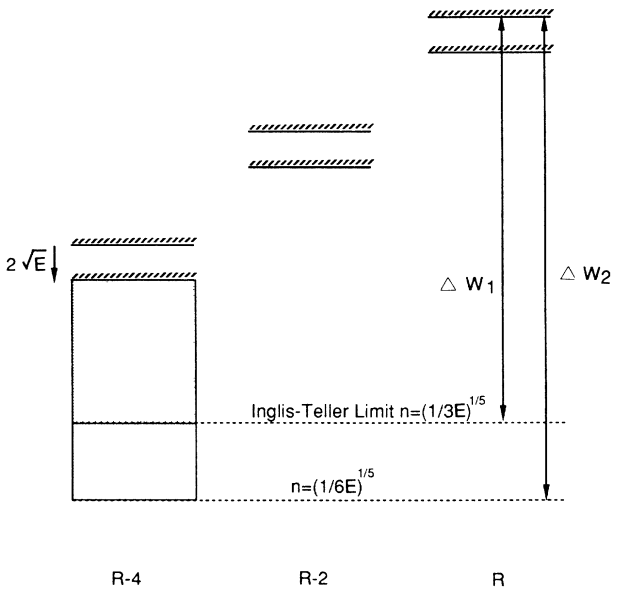

FIG. 6. Schematic of the $v = 0$, R, $R-2$, and $R-4$ ion limits of Li_2^+. In a static field E all three limits are depressed by $2\sqrt{E}$. Also shown are the positions of the Inglis-Teller and $\frac{1}{2}$ Inglis-Teller limits in the $R-4$ series which correspond to the threshold shifts of Eqs. (14) and (16), and Eqs. (15) and (17), respectively.

V. COMPARISON OF THEORY TO EXPERIMENT

We wish to compare our data, which we have expressed as threshold shifts, to the theoretical model proposed in the preceding section. For autoionization to occur, two requirements must be met. First, forced autoionization must depress the limit below the initially populated Rydberg state, and, second, the angular momentum barrier must be eliminated. Taking these two requirements into account, it is clear that, for any given field, the threshold shift is the lesser of the shifts implied by Eqs. (1) and (14). For low R the shift is determined by the forced autoionization criterion, Eq. (1), and for high

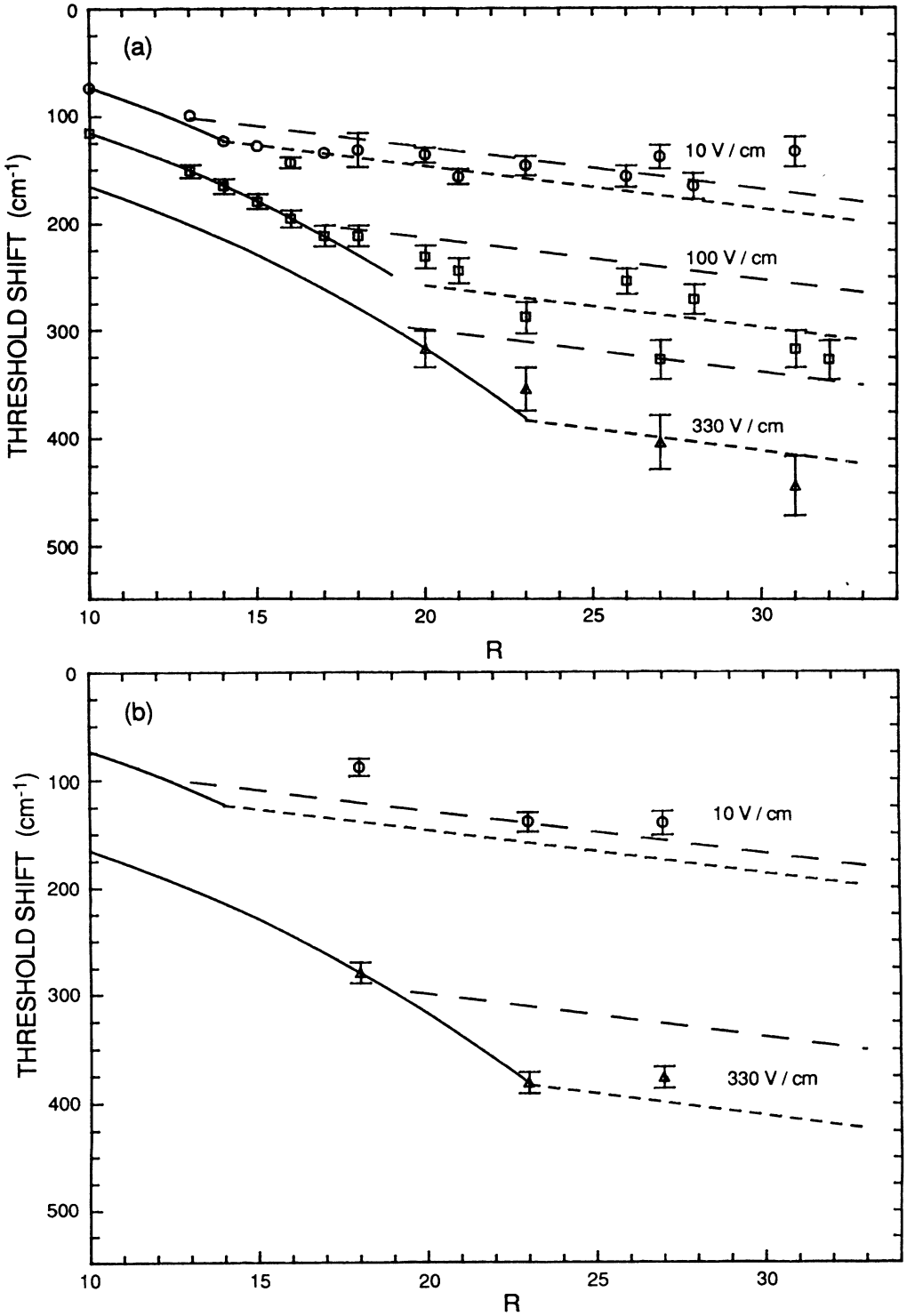

FIG. 7. Threshold shift data of (a) Table I for $v=0$ and (b) Table II for $v=1$ excluding vibrational energy. Included are the theories of Eq. (1) (solid line), Eq. (14) (long-dashed line), and Eq. (16) (short-dashed line).

R by the angular momentum barrier reduction requirement, Eq. (14). We note that Eq. (14), which requires that the Stark shifts of the Rydberg series converging to the $R-4$ limit span the entire Δn interval, gives a lower limit for the threshold shift. On the average a better requirement would be that the Stark levels fill half the Δn interval. This leads to a depression of the limit below the zero-field R ionization limit by

$$\Delta W_2 = 8B_0R - 4B_0 + \tfrac{1}{2}(6E)^{2/5} . \quad (16)$$

Similarly, Eq. (15) becomes

$$I(0) + (R-4)(R-3)B_0 - W = \tfrac{1}{2}(6E)^{2/5} . \quad (17)$$

To compare our experimental data of Table I to Eqs. (14) and (16) we need to connect J' of the intermediate A state to R of Eqs. (14) and (16). First we note that we excite primarily $l=2$ Rydberg states, and $J=J'$, $J'\pm1$ are allowed final angular momenta. For $l=2$, $J'-3 \le R \le J'+3$. Of these values of R the most likely to autoionize is a Rydberg state converging to the $R=J'-3$ limit. We therefore use $R=J'-3$ to fit the data of Table I to Eqs. (14) and (16).

In Fig. 7(a) we have plotted the threshold shifts of the Rydberg states converging to the $v=0$ levels of the ion as a function of R of the ionic level. We have also plotted the theoretical curves corresponding to Eqs. (1), (14), and (16) for comparison. As previously shown by Janik *et al.*,[2] for low R the threshold shifts are determined by the forced autoionization criterion. This point is shown here explicitly by the 100 V/cm data of Fig. 7(a) for $R \le 18$. For high R the data all lie below the solid line corresponding to Eq. (14), consistent with its being a lower limit to the depression of the limit. The data are, however, in excellent agreement with the dashed line corresponding to Eq. (16), which should give a better estimate of the depression of the limit.

We can also compare our data for the Rydberg states converging to $v=1$ levels of the ion core to the model. This comparison can be expected to be meaningful if, as proposed by Bordas *et al.*,[4,5] vibrational-rotational autoionization occurs at a rate similar to that of pure rotational autoionization. Specifically the mechanism we propose is a $\Delta v=-1$, $\Delta R=-2$, $\Delta l=2$ transition followed by a series of $\Delta v=0$, $\Delta R=-2$, $\Delta l=0$ transitions as in the case of the Rydberg series converging to the $v=0$ levels of the ion. In Fig. 7(b) we show the data of Table II and the theoretical curves corresponding to Eqs. (1), (14), and (16), excluding the $\Delta v=-1$ vibrational energy transfer in the threshold shift.

In Fig. 8 we plot the $v=1$ field threshold data of Table III along with the theory of Eqs. (15) and (17). For these states, however, we can no longer exclusively assume $R=J'=-3$ in Eqs. (15) and (17). Recall that in general $J=J'-1$, J', and $J''+1$ corresponding to the P, Q, and R Rydberg $\leftarrow A$ transitions, respectively. We recall also that Rydberg states with $\Delta R=\pm2$ and the same J are strongly coupled by their quadrupole interaction with the core. Of these states, the ones most likely to autoionize are those with the lowest R, which, for $l=2$ states, are

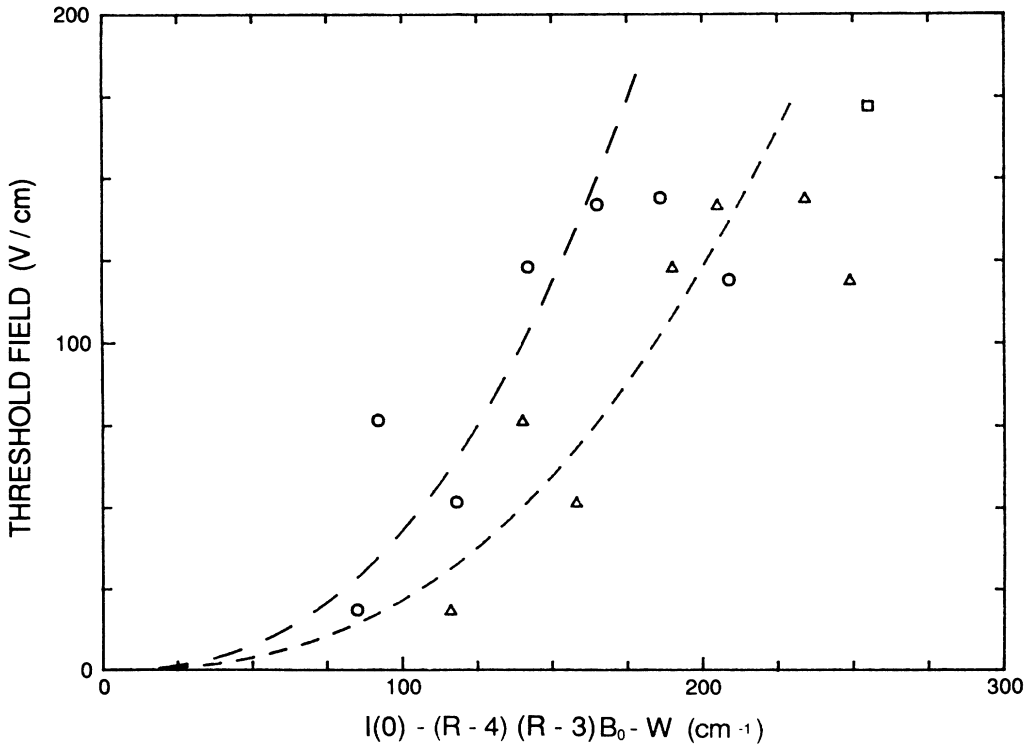

FIG. 8. Field threshold data of Table III plotted with $R=J'-3$ (circles), $R=J'-2$ (squares) and $R=J'-1$ (triangles). Included are the theories of Eqs. (15) (long-dashed line) and (17) (short-dashed line).

$R = J' - 3$, $J' - 2$, or $J' - 1$ for states with $J = J' - 1$, J', and $J' + 1$, respectively. For the states of Table III that are assigned as either $R = J' + 1$ or $J' - 1$, we therefore use both minimum R values of $R = J' - 3$ or $J' - 1$ in Eqs. (15) and (17). Similarly, for the state assigned in Table III as $R = J'$ we use $R = J' - 2$.

As shown by Figs. 7(b) and 8 the $v = 1$ data match the model approximately as well as in Fig. 7(a), indicating that this picture of the autoionization process is correct for vibrational-rotational autoionization as well as pure rotational autoionization.

VI. CONCLUSION

Here we have reported a systematic set of measurements which shows that the rotational autoionization of a diatomic molecule is dramatically affected by small electric fields. Our measurements agree well with a model based on two distinct effects, forced autoionization, and the removal of an angular momentum impediment to autoionization of Rydberg states converging to high rotational levels of the ion. Forced autoionization has been well studied in atomic systems. In contrast, there are no atomic analog to the Rydberg states converging to the high rotational levels of the ion, and the removal of the angular momentum barrier is a purely molecular phenomenon.

ACKNOWLEDGMENTS

It is a pleasure to acknowledge stimulating discussions with R. R. Jones, O. C. Mullins, W. Sandner, and J. Berkowitz during the course of this work, which has been supported by the National Science Foundation under Grant No. PHY-8619056.

*Present address: Jet Propulsion Laboratory, 4800 Oak Grove Dr., Pasadena, CA 91109.

[1]W. Sandner, K. A. Safinya, and T. F. Gallagher, Phys. Rev. A **33**, 1008 (1986).

[2]G. R. Janik, O. C. Mullins, C. R. Mahon, and T. F. Gallagher, Phys. Rev. A **35**, 2345 (1987).

[3]E. Y. Xu, H. Helm, and R. Kachru, Phys. Rev. A **38**, 1666 (1988).

[4]C. Bordas, M. Broyer, P. Labastie, and B. Tribollet, in *Photophysics and Photochemistry Above 6 eV,* edited by F. Lahmani (Elsevier, Amsterdam, 1985).

[5]C. Bordas, P. Brevet, M. Broyer, J. Chevaleyre, and P. Labastie, Europhys. Lett. **3**, 789 (1987).

[6]D. Eisel and W. Demtröder, Chem. Phys. Lett. **88**, 481 (1982).

[7]R. A. Bernheim, L. P. Gold, and T. Tipton, J. Chem. Phys. **78**, 3635 (1983).

[8]E. E. Eyler and F. M. Pipkin, Phys. Rev. A **27**, 2462 (1983).

[9]S. M. Jaffe, R. Kachru, H. B. van Linden van den Heuvell, and T. F. Gallagher, Phys. Rev. A **32**, 1480 (1985).

[10]D. M. Bishop and C. Pouchan, Chem. Phys. Lett. **102**, 132 (1983).

[11]H. A. Bethe and E. E. Salpeter, *Quantum Mechanics of One- and Two-Electron Atoms* (Plenum, New York, 1977).

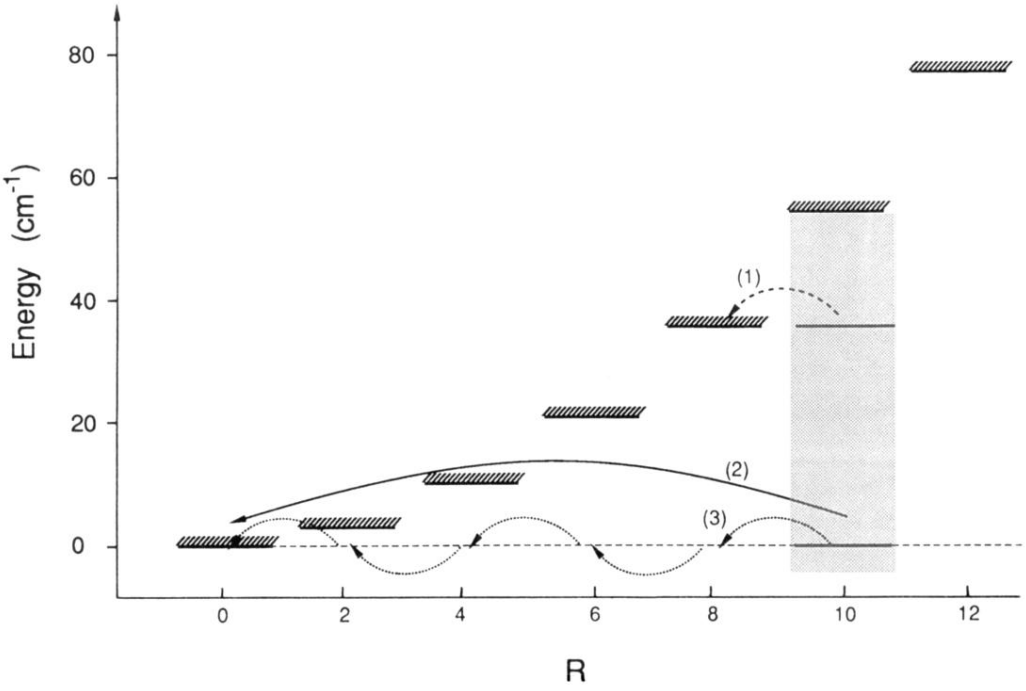

FIG. 5. Schematic showing the positions of the $R=0$–12, $v=0$ limits of Li_2^+ relative to the lowest $v=0$, $R=0$ limit. Rydberg states converging to the $R=10$ limit that lie above the $R=8$ limit may autoionize by a single $\Delta R=-2$, $\Delta Rl=+2$ quadrupole transition with observable rate $>10^7\ s^{-1}$ [path (1)]. Lower-lying states just above the $R=0$ limit may autoionize to the $R=0$ continuum essentially in two ways. The first is via their $\Delta R=-2$, $\Delta l=+2$ quadrupole couplings with the nearly degenerate states of the four intermediate Rydberg series [path (3)]. The second is the direct 2^{10}-pole, $\Delta R=-10$, $\Delta=+10$ process [path (2)].

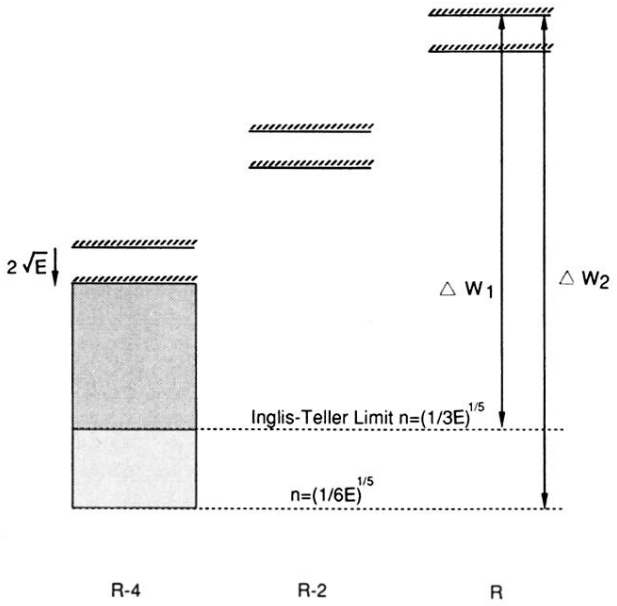

FIG. 6. Schematic of the $v=0$, R, $R-2$, and $R-4$ ion limits of Li_2^+. In a static field E all three limits are depressed by $2\sqrt{E}$. Also shown are the positions of the Inglis-Teller and $\frac{1}{2}$ Inglis-Teller limits in the $R-4$ series which correspond to the threshold shifts of Eqs. (14) and (16), and Eqs. (15) and (17), respectively.